

PLUMBERS' KNOTS

CHAD GIUSTI

We describe a new version of finite-complexity knot theory in \mathbb{R}^3 and we resolve the fundamental questions about enumerating and distinguishing knot types in this theory. We further show that these knot spaces stabilize to a space with the components of the classical knot space, indicating that our results could lead to fundamental progress in that area as well.

The curves we consider, called plumbers' curves, are piecewise linear (hereafter, PL) curves which are restricted so that the image of each linear map is parallel to one of the coordinate axes and so that these axes alternate in a fixed order. The collection of all such curves decomposes into a directed system of spaces P_n of *plumbers' curves of n moves*, each of which is homeomorphic to a Euclidean cube. Inside of each P_n lies the space of *plumbers' knots of n moves*, K_n , whose set of components converges to that of the space of C^1 (long) knots. As such, these spaces provide us with a model for classical knot theory, one application of which will be our construction of an unstable Vassiliev spectral sequence in [3].

We begin by showing that each plumbers' curve space P_n admits a cell decomposition whose structure can be canonically encoded through elementary combinatorics. Within this cell complex we identify a subcomplex for $S_n = P_n \setminus K_n$, the space of singular curves. Understanding this subcomplex allows us to construct a deterministic finite-time algorithm that enumerates the components of K_n .

An implementation of this algorithm has demonstrated that there are seven knot types in K_5 , forty-nine in K_6 . The seven components of K_5 correspond, topologically, to the unknot, three right-handed trefoils and three left-handed trefoils. This phenomenon of “stuck knots”, knots which are not isotopic at a level of finite complexity but whose topological isotopy classes coincide, was observed for PL knots by Calvo [2].

Plumbers' knots bear strong resemblance to both lattice knots as considered, for example, in [4], and the cubical diagrams studied in [1]. We observe that a plumbers' knot can be viewed as a particular lattice knot, and put bounds on number of the classes of lattice knots that arise in each P_n . The similarity to the cubical diagrams of Baldridge and Lowrance [1] suggests that the tools we develop for plumbers' knots could be useful in the study of knot Floer homology.

The author would like to thank his advisor, Dev Sinha, for the countless hours of conversation and support without which this research would not have been possible.

1. PLUMBERS' CURVES

We begin by introducing plumbers' curves and the terminology we will use to study them.

Fix a basis $\{x, y, z\}$ for \mathbb{R}^3 . Let \mathbb{I}^3 be the cube $[0, 1]^3 \subseteq \mathbb{R}^3$ and $P_n = (\text{Int } \mathbb{I}^3)^{n-1}$. Given a point $v \in P_n$, we construct a map $\phi_v : \mathbb{R} \rightarrow \mathbb{R}^3$ with support on the interval $[0, 3]$ which we call a *plumbers' curve* with $3n$ “sections of pipe”.

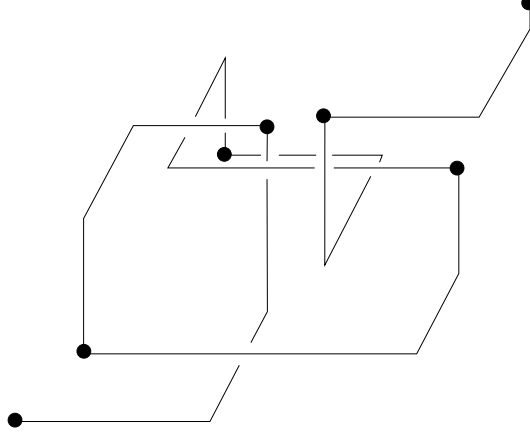


FIGURE 1. A plumbers' curve of 6 moves.

Definition 1.1. Let $v = (v_0, v_1, \dots, v_n) \in P_n$ with $v_0 = (0, 0, 0)$ and $v_n = (1, 1, 1)$. For $i \in \{0, \dots, n-1\}$, define maps which interpolate between consecutive v_i in three steps, parallel to the coordinate axes, as follows.

$$\begin{aligned} \mathbf{x}_i(t) : \left[\frac{3i}{n}, \frac{3i+1}{n} \right] &\rightarrow \mathbb{R}^3 &= ((3i+1-nt)v_i^x + (nt-3i)v_{i+1}^x, v_i^y, v_i^z) \\ \mathbf{y}_i(t) : \left[\frac{3i+1}{n}, \frac{3i+2}{n} \right] &\rightarrow \mathbb{R}^3 &= (v_{i+1}^x, (3i+2-nt)v_i^y + (nt-3i-1)v_{i+1}^y, v_i^z) \\ \mathbf{z}_i(t) : \left[\frac{3i+2}{n}, \frac{3i+3}{n} \right] &\rightarrow \mathbb{R}^3 &= (v_{i+1}^x, v_{i+1}^y, (3i+3-nt)v_i^z + (nt-3i-2)v_{i+1}^z) \end{aligned}$$

Each such map is a *pipe*, and we will sometimes not distinguish between such and its image. Set the *length* of \mathbf{x}_i as $\|\mathbf{x}_i\| = |\mathbf{x}_i(\frac{3i}{n}) - \mathbf{x}_i(\frac{3i+1}{n})|$, and its *direction* to be

$$s(\mathbf{x}_i) = \begin{cases} 1 & \mathbf{x}_i(\frac{3i}{n}) > \mathbf{x}_i(\frac{3i+1}{n}) \\ 0 & \mathbf{x}_i(\frac{3i}{n}) = \mathbf{x}_i(\frac{3i+1}{n}) \\ -1 & \mathbf{x}_i(\frac{3i}{n}) < \mathbf{x}_i(\frac{3i+1}{n}). \end{cases}$$

Make similar definitions for \mathbf{y}_i and \mathbf{z}_i .

Let $\phi_v(t) : [0, 3] \rightarrow \mathbb{I}^3$ be the union of these maps. We call ϕ_v an *n-move plumbers' curve*. An example of such a curve is given in Figure 1

These maps encode piecewise linear motion parallel to the x -, y - and z -axes. A generic curve alternates these three directions of motion in the order x, y, z, x, \dots, z . Further, up to reparametrization any such map is obtainable via such a construction, so we can identify P_n with the space of such curves, and call P_n the *space of n-move plumber's curves*. Unless we are specifically using the properties of the map ϕ_v , we will make most of our statements about the underlying point v .

There are two types of singularities in C^1 curves: transverse self-intersection and points at which the derivative vanishes. However, the more rigid nature of plumbers' curves reduces these to a single condition, which we will readily be able to detect.

Definition 1.2. We say two pipes are *distant* if they are separated by at least three intervening pipes. For example, \mathbf{x}_i and \mathbf{x}_{i+1} are not distant, but \mathbf{x}_i and \mathbf{y}_{i+1} are.

A non-singular plumbers' curve is a *plumbers' knot*, and the space of all such is $K_n \subseteq P_n$. The *discriminant* $S_n = P_n \setminus K_n$ is the subspace of singular plumbers' curves.

Definition 1.3. Let $\phi_v, \phi_w \in K_n$. We say ϕ_v and ϕ_w are *geometrically isotopic* if there is a path $\Phi_{v,w} : \mathbb{I} \rightarrow K_n$ with $\Phi_{v,w}(0) = v$ and $\Phi_{v,w}(1) = w$.

Later, we will see that the notion geometric isotopy in any K_n is stronger than the usual topological notion of knot isotopy. However, the two notions converge as we increase the articulation of plumbers' knots. The fact that geometric isotopies preserve the number of moves in a knot will be the fundamental component in our solutions of the problems of enumerating and distinguishing plumbers' knots.

2. A CELL COMPLEX FOR S_n

We will now make a crucial observation: the spaces P_n possess an intrinsic combinatorial cell structure which is compatible with the partition into subspaces S_n and K_n .

Let Σ_n be the symmetric group on n letters. It will sometimes be convenient to represent $\sigma \in \Sigma_n$ in *permutation* notation, $\sigma(1)\sigma(2)\dots\sigma(n)$. By convention, we will use τ exclusively to refer to transpositions, while other symbols may represent any permutation.

As most of our constructions and results will be symmetric for our x , y and z coordinates, we will often make statements only for x .

Definition 2.1. Let $\sigma \in \Sigma_{n-1}$. We say $v \in P_n$ *respects* σ in x if

$$(1) \quad 0 < v_{\sigma_i(1)}^x < v_{\sigma_i(2)}^x < \dots < v_{\sigma_i(n-1)}^x < 1$$

Let $\sigma_x, \sigma_y, \sigma_z \in \Sigma_{n-1}$. Define a cell in P_n by

$$e(\sigma_x, \sigma_y, \sigma_z) = \{v \in P_n \mid v \text{ respects } \sigma_x \text{ in } x, \sigma_y \text{ in } y \text{ and } \sigma_z \text{ in } z\}$$

When we write the permutations in permutation notation, the name of the cell transparently describes the defining inequalities. Such cells are a product of three $(n-1)$ -simplices. Let $\text{CELL}_\bullet(P_n)$ be the cellular chain complex associated to this decomposition, which thus computes the homology of P_n .

Each top-dimensional cell described above is non-empty. We distinguish an element as follows.

Definition 2.2. Given a cell $e = e(\sigma_x, \sigma_y, \sigma_z) \subseteq P_n$, construct an n -move plumbers' knot by choosing the point $v(e)$ in the cell given by

$$v(e)_i = \left(\frac{\sigma_x^{-1}(i)}{n}, \frac{\sigma_y^{-1}(i)}{n}, \frac{\sigma_z^{-1}(i)}{n} \right).$$

The knot $\phi_{v(e)}$ is called the *representative knot* for e .

Any plumbers' knot ϕ_v in the closure of a cell is geometrically isotopic to the representative knot for that cell via a straight line geometric isotopy. Thus, to study geometric isotopy types of n -move plumbers' knots it suffices to study only representative knots.

Lemma 2.3. *If a plumbers' curve ϕ_v is singular, v is in the closure of a codimension one cell. Further, if some ϕ_v is singular and $v \in e$, all v in the closure of e are.*

Proof. If ϕ_v is singular, there must be distant pipes a and b which intersect. As the pipes are lines parallel to the coordinate axes, it is easy to characterize plumbers' curves for which given pipes intersect. Here and elsewhere, we “ $(p-r)(q-r) \leq 0$ ” in place of “neither $q < r < p$ nor $q < r < p$ ”. Then

$\mathbf{x}_i \cap \mathbf{y}_j$ if

- (1) $(v_i^x - v_{j+1}^x)(v_{i+1}^x - v_{j+1}^x) \leq 0$,
- (2) $(v_j^y - v_i^y)(v_{j+1}^y - v_i^y) \leq 0$ and
- (3) $v_i^z = v_j^z$,

$\mathbf{x}_i \cap \mathbf{z}_j$ if

- (1) $(v_i^x - v_{j+1}^x)(v_{i+1}^x - v_{j+1}^x) \leq 0$,
- (2) $v_i^y = v_{j+1}^y$ and
- (3) $(v_j^z - v_i^z)(v_{j+1}^z - v_i^z) \leq 0$,

and $\mathbf{y}_j \cap \mathbf{z}_i$ if

- (1) $v_{i+1}^x = v_{j+1}^x$,
- (2) $(v_j^y - v_{i+1}^y)(v_{j+1}^y - v_{i+1}^y) \leq 0$ and
- (3) $(v_i^z - v_j^z)(v_{i+1}^z - v_j^z) \leq 0$.

Each of these conditions requires some equality of the form $v_{i+1}^x = v_{j+1}^x$, $v_i^y = v_{j+1}^y$ or $v_i^z = v_j^z$. As $e(\sigma_x, \sigma_y, \sigma_z)$ is a product of simplices, such are satisfied only on the boundary of a cell. It is clear that if any v in a particular boundary cell of $e(\sigma_x, \sigma_y, \sigma_z)$ satisfies such a condition, all in that cell do so. \square

Lemma 2.3 tells us both that K_n is an open submanifold of P_n and that the discriminant S_n is described by a closed subcomplex of P_n generated by codimension one cells, whose combinatorics we now carefully develop.

Definition 2.4. Let $\sigma \in \Sigma_n$. We say $\tau \in \Sigma_n$ is a *transposition appearing in σ* if it is of the form $\tau = (\sigma(i) \sigma(i+1))$ for some $i \in \{1 \dots n-1\}$.

That is, postcomposing σ by τ exchanges two adjacent letters in permutation notation. For example, the transpositions appearing in 3124 are (3 1), (1 2) and (2 4).

The transpositions appearing in the permutations σ_x, σ_y and σ_z precisely describe the boundaries of the cell $e(\sigma_x, \sigma_y, \sigma_z)$.

Proposition 2.5. *Let $e(\sigma_x, \sigma_y, \sigma_z) \in \text{CELL}_{3n-3}(P_n)$ and τ a transposition. Then $\bar{e}(\sigma_x, \sigma_y, \sigma_z) \cap \bar{e}(\tau\sigma_x, \sigma_y, \sigma_z)$ is of codimension 1 if and only if τ appears in σ_x .*

This motivates the following naming convention for codimension 1 cells.

Definition 2.6. Let $e(\sigma_x, \sigma_y, \sigma_z) \subseteq P_n$ be a cell and $\tau_x = (\sigma_x(i) \sigma_x(i+1))$ a transposition appearing in σ_x . Define a codimension one cell named $e(\sigma_x, \sigma_y, \sigma_z; \tau_x)$ using the same equations as for $e(\sigma_x, \sigma_y, \sigma_z)$ but changing the inequality $v_{\sigma_x(i)}^x < v_{\sigma_x(i+1)}^x$ in equation (1) to an equality.

This notation is redundant; in particular, each cell is named twice. However, this convention makes incidence relations with the $(3n-3)$ -cells easy to understand and identification of duplicate names is straightforward.

Proposition 2.7. $e(\sigma_x, \sigma_y, \sigma_z; \tau_x) = e(\sigma'_x, \sigma_y, \sigma_z; \tau_x)$ if and only if $\tau_x \sigma_x = \sigma'_x$.

We can extend this notation to name cells of any codimension.

Definition 2.8. Let $\ell : \Sigma_n \rightarrow \mathbb{N}$ be the standard length function, $\sigma, \rho \in \Sigma_n$. Say ρ is a permutation appearing in σ if ρ admits a decomposition into $\ell(\rho)$ transpositions, each of which is a transposition appearing in σ .

If ρ appears in σ , then its decomposition into transpositions appearing in σ is unique up to reordering. This occurs because in a decomposition of ρ into disjoint cycles ρ^j , $\sigma(i)$ and $\sigma(i+1)$ occur in the same ρ^j if and only if $(\sigma(i) \sigma(i+1))$ is a transposition in the decomposition of ρ .

Definition 2.9. Let $e(\sigma_x, \sigma_y, \sigma_z) \in \text{CELL}_{3n-3}(P_n)$ and $\rho_x, \rho_y, \rho_z \in \Sigma_{n-1}$ be permutations such that ρ_i appears in $\sigma_i, i \in \{x, y, z\}$. Define $e(\sigma_x, \sigma_y, \sigma_z; \rho_x, \rho_y, \rho_z) \in \text{CELL}_{3n-3-(\ell(\rho_x)+\ell(\rho_y)+\ell(\rho_z))}(P_n)$ by, for each transposition occurring in the chosen decomposition of the ρ_i , changing the appropriate inequality in equation (1) to an equality as in Definition 2.6.

The uniqueness of the decomposition of the ρ shows that this cell naming convention is well defined, as there is only one choice of equalities associated to a given cell name. We can determine how many different names apply to a given cell by examining the ρ .

Proposition 2.10. Let $e(\sigma_x, \sigma_y, \sigma_z; \rho_x, \rho_y, \rho_z) \in \text{CELL}_\bullet(P_n)$. Decompose each $\rho_i, i \in \{x, y, z\}$, into a product of $k(i)$ of disjoint cycles, ρ_i^j . The cell e has

$$\#e = \prod_{i \in \{x, y, z\}} \left[\prod_{j=1}^{k(i)} (\ell(\rho_i^j) + 1)! \right]$$

redundant labels. Each such label uniquely identifies a top dimensional cell in whose closure e occurs.

Proof. Let ρ_x^j be a cycle in the decomposition of ρ_x into disjoint cycles. The requirement that ρ_x^j appear in σ_x tells us that this subset of $\{1, \dots, n-1\}$ on which ρ_x^j has nontrivial action is precisely $\{\sigma(t), \sigma(t+1), \dots, \sigma(t + \ell(\rho_x^j))\}$ for some t . Now, the cell $e(\sigma_x, \sigma_y, \sigma_z; \rho_x^j)$ is defined to be all maps v respecting σ_y in y , σ_z in z and so that

$$0 < v_{\sigma_i(1)}^x < \dots < v_{\sigma_i(t)}^x = v_{\sigma_i(t+1)}^x = \dots = v_{\sigma_i(t+\ell(\rho_x^j))}^x < \dots < v_{\sigma_i(n-1)}^x < 1$$

That is, decomposing ρ_x into disjoint cycles is equivalent to isolating blocks of adjacent of equalities in equation (1).

To select a cell $e(\sigma'_x, \sigma_y, \sigma_z)$ which has in its closure $e(\sigma_x, \sigma_y, \sigma_z, \rho_x^i)$, we choose an order for these vertices. There are $(\ell(\rho_x^j) + 1)!$ such, and it is clear that this choice does not affect the corresponding choices for the other disjoint cycles in ρ_x .

As we can perform this procedure independently for each of the disjoint cycles and for each coordinate, our final count is simply the product of that for the disjoint cycles, as required. \square

For example, there are two classes of names for codimension 2 cells: those for which the ρ are some combination of two disjoint transpositions and those for which the ρ consist of a single 3-cycle. In the former case, there are 4 names for each cell, while in the latter there are 6.

Utilizing this naming scheme, we can extend the idea of representative knots for top dimensional cells to produce representative curves for every cell in $\text{CELL}_\bullet(P_n)$.

Definition 2.11. Fix a cell $e = e(\sigma_x, \sigma_y, \sigma_z; \rho_x, \rho_y, \rho_z) \subseteq P_n$. Recall that ℓ is the length function on permutations. A map in such a cell will have vertices in $n - \ell(\rho_x)$ (y - z)-planes, some of the x vertices now being coplanar. We need to define a function $E[\rho_x](i)$ that counts the number of equalities that occur before v_i in the x -axis equation for e .

Choose an order of the independent cycles in ρ_x so that the elements of $\{1 \dots n\}$ appear in the order $\sigma_x(1), \sigma_x(2), \dots, \sigma_x(n)$, and label the k th cycle in this order $(\rho_x)_k$. For example, if $\sigma_x = 312546$ and $\rho_x = (45)(123)$, we would rewrite ρ_x as $(312)(54)(6)$ with $(\rho_x)_1 = (312)$, $(\rho_x)_2 = (54)$ and $(\rho_x)_3 = (6)$. Now, define $E[\rho_x](i)$ to be the map which returns the subscript of the cycle in which i apperas.

Construct an n -move plumbers' curve $\phi_{v(e)} \in e$ by

$$v(e)_i = \left(\frac{E[\rho_x](i)}{n - \ell(\rho_x)}, \frac{E[\rho_y](i)}{n - \ell(\rho_y)}, \frac{E[\rho_z](i)}{n - \ell(\rho_z)} \right).$$

The knot $\phi_{v(e)}$ is called the *representative curve* (or *knot*) for e .

2.1. An algorithm for computing components of K_n . Our naming convention for cells allows us to resolve several fundamental questions about the spaces of plumbers' knots algorithmically.

By Lemma 2.3, there are two types of codimension 1 cells: those which consist of plumbers' knots and those which consist of singular plumbers' curves. As those which consist of singular plumbers' curves generate a cell complex for S_n , we wish to distinguish them. Fortunately, we can determine combinatorially into which of these classes a given cell falls.

Choose the representative knot for a cell $e(\sigma_x, \sigma_y, \sigma_z)$ and a transposition $\tau = (\sigma_x(i) \ \sigma_x(i+1)) = (a \ b)$ appearing in σ_x . Geometrically, applying τ to σ_x corresponds to exchanging the x -coordinates of the a th and b th vertices, which "pushes" the $(y$ - z)-plane $x = \frac{i}{n}$ past the $(y$ - z)-plane $x = \frac{i+1}{n}$. As they lie in the plane $x = \frac{i}{n}$, this forces the pipes \mathbf{y}_{a-1} and \mathbf{z}_{a-1} to move, possibly intersecting \mathbf{z}_{b-1} or \mathbf{y}_{b-1} respectively, as illustrated in Figure 2. While an intersection between other pipes than those mentioned is possible, this always occurs in addition to one of the singularities mentioned above.

A similar analysis demonstrates that transpositions appearing in σ_y (respectively, σ_z) can only cause intersections of the form $\mathbf{x}_a \cap \mathbf{z}_{b-1}$ or $\mathbf{x}_b \cap \mathbf{z}_{a-1}$ (respectively, $\mathbf{x}_a \cap \mathbf{y}_b$ or $\mathbf{x}_b \cap \mathbf{y}_a$).

Definition 2.12. Let $e(\sigma_x, \sigma_y, \sigma_z)$ be a cell in P_n , $\tau_x = (a \ b)$ a transposition appearing in σ_x . We say that τ_x *produces an intersection* if one of the following pairs of conditions holds.

Either

- (1) $\sigma_y^{-1}(b)$ is between $\sigma_y^{-1}(a-1)$ and $\sigma_y^{-1}(a)$ and $\sigma_z^{-1}(a-1)$ is between $\sigma_z^{-1}(b-1)$ and $\sigma_z^{-1}(b)$
- (2) $\sigma_y^{-1}(a)$ is between $\sigma_y^{-1}(b-1)$ and $\sigma_y^{-1}(b)$ and $\sigma_z^{-1}(b-1)$ is between $\sigma_z^{-1}(a-1)$ and $\sigma_z^{-1}(a)$

This condition is precisely that for $\mathbf{y}_j \cap \mathbf{z}_i$ in the proof of Lemma 2.3. The definitions for y and z are similar.

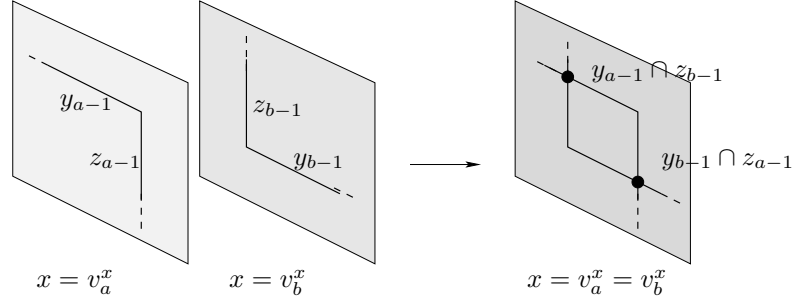


FIGURE 2. Transposing x-coordinates may result in y-z intersections.

Theorem 2.13. *Let $e(\sigma_x, \sigma_y, \sigma_z)$ and τ_x be as in Definition 2.12. There is a straight-line geometric isotopy between the representative knots for $e(\sigma_x, \sigma_y, \sigma_z)$ and $e(\tau_x \sigma_x, \sigma_y, \sigma_z)$ if and only if τ_x does not produce a y-z intersection.*

If an isotopy such as the one in the theorem exists, it is an *elementary geometric isotopy*. Elementary geometric isotopies play a role for plumbers' knots similar to that played by Reidemeister moves for C^1 knots. We notice, however, that unlike Reidemeister moves, elementary geometric isotopies preserve the complexity of the knot, as measured in number of moves necessary to represent it. This allows us to consider the equivalence relation generated by such in an explicit fashion.

Corollary 2.14. *Let $\phi_v, \phi_w \in K_n$, $v \in e(\sigma_x, \sigma_y, \sigma_z)$, $w \in e(\sigma'_x, \sigma'_y, \sigma'_z)$. ϕ_v is geometrically isotopic to ϕ_w if and only if there is a sequence of elementary geometric isotopies connecting the representative knots for $e(\sigma_x, \sigma_y, \sigma_z)$ and $e(\sigma'_x, \sigma'_y, \sigma'_z)$.*

Corollary 2.15. $H_0(K_n) \cong \mathbb{Z}\langle e(\sigma_x, \sigma_y, \sigma_z) \mid \sigma_x, \sigma_y, \sigma_z \in \Sigma_{n-1} \rangle / \sim$, where \sim is the equivalence relation generated by elementary geometric isotopies.

As an application of Corollary 2.15, we can computationally determine if two n -move plumbers' knots ϕ_v and $\phi_{v'}$ are geometrically isotopic. Without loss of generality, v and v' occur in the interior of a $(3n-3)$ -cell.

Algorithm 2.16. (1) Construct a graph (V, E) with $V = \text{CELL}_{3n-3}(P_n)$ and $(e, e') \in E$ if there is an elementary geometric isotopy between the representative knots for e and e' .
 (2) Let $e_0, e_1 \in V$ with $v \in e_0$, $v' \in e_1$.
 (3) Starting at e_0 , perform a graph search for e_1 . Such a search recursively traverses edges in the graph until it either locates e_1 or exhausts all vertices in its component. If the search terminates successfully, the knots are isotopic. Otherwise, they are not geometrically isotopic for the given n .

If it is possible to determine into which K_n a plumbers' knot must be embedded to ensure that geometric isotopy coincides with isotopy, Algorithm 2.16 will thus determine if given knots are isotopic in $O((n!)^3)$ running time.

A modified version of Algorithm 2.16 which instead simply identifies the components of the graph actually enumerates the geometric isotopy classes of K_n . The results of this algorithm being run on K_5 and K_6 are included in Table 1. The topological isotopy classes of these knots were determined by computation of known knot invariants on representatives of each class. The code for each of these processes is appended to the end of the \LaTeX file for this paper on the arXiv.

Components of K_5				
Type	Cells	Representative	Type	Representative
0_1	13,728	$[1234_x, 1234_y, 1234_z]$		
3_1 (R)	31	$[1342_x, 2413_y, 2413_z]$	3_1 (L)	$[1342_x, 3142_y, 2413_z]$
	16	$[1342_x, 2413_y, 3124_z]$		$[1342_x, 3142_y, 3124_z]$
	1	$[2431_x, 2413_y, 4213_z]$		$[2431_x, 3142_y, 4213_z]$
Components of K_6				
0_1	1,687,172	$[12345_x, 12345_y, 12345_z]$		
3_1 (R)	19507	$[24135_x, 31245_y, 23145_z]$	3_1 (L)	$[12453_x, 13524_y, 13524_z]$
	5	$[42351_x, 24315_y, 24135_z]$		$[42351_x, 51342_y, 24135_z]$
	5	$[13524_x, 15324_y, 51342_z]$		$[13524_x, 42351_y, 51342_z]$
4_1	393	$[14352_x, 31452_y, 42135_z]$	4_1	$[31452_x, 31524_y, 32451_z]$
	393	$[24153_x, 25314_y, 24315_z]$		$[24513_x, 42135_y, 32415_z]$
5_1 (R)	19	$[24153_x, 31524_y, 42315_z]$	5_1 (L)	$[15342_x, 31542_y, 31524_z]$
	19	$[25134_x, 41253_y, 35241_z]$		$[52413_x, 24513_y, 25314_z]$
	4	$[15342_x, 24153_y, 42153_z]$		$[15342_x, 31542_y, 42513_z]$
	4	$[31542_x, 31524_y, 42315_z]$		$[31542_x, 42513_y, 42315_z]$
	1	$[41523_x, 41352_y, 34152_z]$		$[41523_x, 25314_y, 34152_z]$
5_2 (R)	12	$[15342_x, 24513_y, 35124_z]$	5_2 (L)	$[15342_x, 31542_y, 35124_z]$
	12	$[25413_x, 35124_y, 25314_z]$		$[24513_x, 42153_y, 42315_z]$
	9	$[25134_x, 24153_y, 35241_z]$		$[25134_x, 35124_y, 35241_z]$
	9	$[25413_x, 31524_y, 42315_z]$		$[52413_x, 24513_y, 23514_z]$
	4	$[15342_x, 24513_y, 42153_z]$		$[15342_x, 31542_y, 42153_z]$
	4	$[31542_x, 31524_y, 42351_z]$		$[31542_x, 42153_y, 42315_z]$
	3	$[15342_x, 25413_y, 31524_z]$		$[15342_x, 31452_y, 31524_z]$
	3	$[24153_x, 35214_y, 42315_z]$		$[24153_x, 41253_y, 42315_z]$
	2	$[15342_x, 25413_y, 42513_z]$		$[15342_x, 31452_y, 42513_z]$
	2	$[35142_x, 35214_y, 42315_z]$		$[35142_x, 41253_y, 42315_z]$
	1	$[15342_x, 24153_y, 41253_z]$		$[15342_x, 35142_y, 41253_z]$
	1	$[31452_x, 31524_y, 42315_z]$		$[31452_x, 42513_y, 42315_z]$
	1	$[41523_x, 25314_y, 43152_z]$		$[41523_x, 41352_y, 43152_z]$
	1	$[41532_x, 41352_y, 34152_z]$		$[41532_x, 25314_y, 34152_z]$

TABLE 1. Components of K_5 and K_6 ; the number of cells in a component are the same in the second column

An immediate consequence of Theorem 2.13 and Lemma 2.3, we have the following characterization of the cell complex for S_n .

Corollary 2.17. *$\text{CELL}_\bullet(S_n)$ is generated in dimension $3n - 4$ as a cell complex by all cells of the form $e(\sigma_x, \sigma_y, \sigma_z, \tau_x)$ for which τ_x produces an intersection.*

Thus, a byproduct of the aforementioned modification to Algorithm 2.16 is an enumeration of the cells in $\text{CELL}_{3n-4}(S_n)$.

3. THE DIRECTED SYSTEM OF SPACES OF PLUMBERS' CURVES AND KNOTS

For fixed n , elements of P_n are too rigid to properly model classes of C^1 knots. Therefore, we require a mechanism by which to increase the articulation of a knot of interest in a fashion which varies continuously across each P_n . As we will also wish

to work with the discriminant, it is convenient to construct the maps $P_n \rightarrow P_{n+1}$ so that they take S_n to S_{n+1} and K_n to K_{n+1} . It would also be useful for the map to be cellular with respect to the cell complex structure on P_n , and we will be able to accomplish this using a “barycentric subdivision” for the majority of the maps in each space. The remainder will be forced to map into the interior of cells, but we will be able to identify in which cells the images are contained.

Occasionally it will be useful to refer to our basis vectors $\{x, y, z\}$ as $\{e_0, e_1, e_2\}$ although this often decreases readability and we will avoid it where possible. When we write $[n]_3$ we are referring to the reduction of n modulo 3.

We require two more pieces of notation in order to understand how the maps in the directed system interact with the cell complex. In particular, we need to build new permutations that reflect the insertion of vertices into the plumbers' maps.

Definition 3.1. Let $k \in \{1 \dots n-1\}$ and $\sigma \in \Sigma_{n-1}$. Define $j_{k,k+1}(\sigma) \in \Sigma_n$ in two steps. First, increase by one the image of the elements of the permutation whose image is already greater than k . For example, if $k = 2$, 12453_x becomes 12564_x . Write the new permutation as $\hat{\sigma}[k]$, defined by

$$\hat{\sigma}[k](i) = \begin{cases} \sigma(i) & \sigma(i) \leq k \\ \sigma(i) + 1 & \sigma(i) > k. \end{cases}$$

Now, insert $k+1$ in the “middle”, lexicographically, of k and $k+2$, so in the above example we end up with 125364_x . Let $a = \min\{\sigma^{-1}(k), \sigma^{-1}(k+1)\}$ and define

$$j_{k,k+1}(\sigma)(i) = \begin{cases} \hat{\sigma}[k](i) & i < \sigma^{-1}(a) + \lfloor \frac{1}{2}(\sigma^{-1}(k) + \sigma^{-1}(k+1)) \rfloor \\ k+1 & i = \sigma^{-1}(a) + \lfloor \frac{1}{2}(\sigma^{-1}(k) + \sigma^{-1}(k+1)) \rfloor \\ \hat{\sigma}[k](i-1) & i > \sigma^{-1}(a) + \lfloor \frac{1}{2}(\sigma^{-1}(k) + \sigma^{-1}(k+1)) \rfloor. \end{cases}$$

Alternately, define an element $j_k(\sigma)$ by inserting $k+1$ immediately following k . In the current example, the result would be 123564_x .

$$j_k(\sigma)(i) = \begin{cases} \hat{\sigma}[k](i) & i < \sigma^{-1}(k) + 1 \\ k+1 & i = \sigma^{-1}(k) + 1 \\ \hat{\sigma}[k](i-1) & i > \sigma^{-1}(k) + 1 \end{cases}$$

We abuse terminology to call the product of the barycentric subdivisions of each of the simplices in a cell again barycentric subdivision. In order to name the subdivided cells in the image, we use the following notation.

$$e(\sigma_x, \sigma_y, \sigma_z; \langle j \rangle_x) = \{v \in e(\sigma_x, \sigma_y, \sigma_z) \mid v_j^x = \frac{1}{2}(v_{\sigma_x(\sigma_x^{-1}(j)-1)}^x + v_{\sigma_x(\sigma_x^{-1}(j)+1)}^x)\}$$

The codimension one subset of the simplex represented by σ_x in which v_j^x is the average of its two neighboring coordinates is a union of faces in the barycentric subdivision, as in Figure 3. Thus, the cell $e(\sigma_x, \sigma_y, \sigma_z; \langle j \rangle_x)$ is a product of the simplices represented by σ_y and σ_z with these faces. Since this set is a subset of an existing cell, we can use our transposition notation for faces in the usual fashion.

Schematically, we want our sequence of maps to insert new vertices in a “sufficiently distributed” fashion across the pipes in a plumbers' curve. To choose the

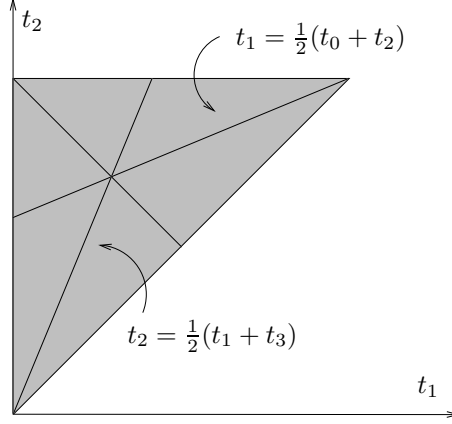


FIGURE 3. Averages of coordinates in barycentric subdivision; here, $t_0 = 0$ and $t_3 = 1$

pipe into which to insert a vertex at each stage, fix a function $\alpha : \mathbb{N} \rightarrow \mathbb{N}$ and insert a vertex into the middle of the a pipe travelling in the $e_{[n]_3}$ direction in the $\alpha(n)$ th move, per Figure 4. For example, choose α so that each move in a map in P_N , for some fixed N , will be chosen in lexicographic order, skipping any newly created moves until vertices have been inserted in each of the existing N pipes, then begin again at P_{2N} .

We can now define the maps on both the pointwise and cellular level in parallel. Let $v \in P_n$ so that there is at least one vertex between v_α and $v_{\alpha+1}$ along the $e_{[n]_3}$ axis. Such points live in cells for which $(\alpha \alpha+1)$ does not appear in $\sigma_{e_{[n]_3}}$. Any cell in with this property will be called *good*.

Definition 3.2. For $n > 2$ and $v \in e \in \text{CELL}_\bullet(P_n)$ with e a good cell, $\alpha = \alpha(n) + 1$ and $\delta_{i,j}$ the Kronecker delta. Define $\iota_n^{\text{good}} : P_n \rightarrow P_{n+1}$ by

$$(\iota_n^{\text{good}}(v))_i = \begin{cases} v_i & i \leq \alpha \\ v_{i-1} & i > \alpha + 1 \end{cases}$$

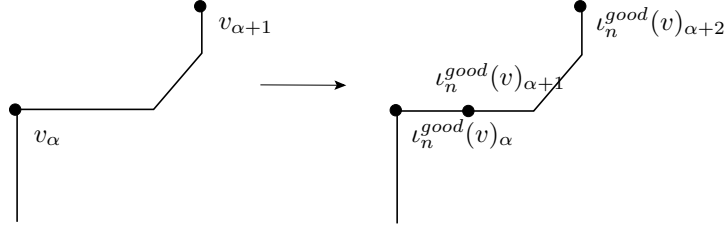
and

$$\begin{aligned} (\iota_n^{\text{good}}(v))_{\alpha+1}^x &= v_{\alpha+1}^x - \frac{1}{2}s(\mathbf{x}_\alpha)||\mathbf{x}_\alpha||\delta_{[n]_3,0} \\ (\iota_n^{\text{good}}(v))_{\alpha+1}^y &= v_\alpha^y + \frac{1}{2}s(\mathbf{y}_\alpha)||\mathbf{y}_\alpha||[n-1]_3 \\ (\iota_n^{\text{good}}(v))_{\alpha+1}^z &= v_\alpha^z + \frac{1}{2}s(\mathbf{z}_\alpha)||\mathbf{z}_\alpha||\delta_{[n]_3,2}. \end{aligned}$$

The image of $\phi_{\iota_n^{\text{good}}(v)}$ is the same as that of ϕ_v , but the curve contains a new vertex which is coplanar in two dimensions with vertices from the old curve and whose third coordinate is the average of the two endpoints of the pipe. This is homotopic to a curve in which the third coordinate is inserted instead at the average of those of the two vertices closest to the middle of the pipe.

Observe that with this definition ι_n^{good} is not cellular, but is cellular when we barycentrically subdivide the codomain. This allows us to use the j maps of Definition 3.1 to determine the image of the cell.

Lemma 3.3. *Let $e \in \text{CELL}_\bullet(P_n)$ be a good cell. Then the image of e under the induced chain map $(\iota_n^{\text{good}})_\#$ is*

FIGURE 4. $\iota_n^{good}(v)$

$$(\iota_n^{good})_{\#}(e(\sigma_x, \sigma_y, \sigma_z)) = e(j_{\alpha, \alpha+1}\sigma_x, j_{\alpha}\sigma_y, j_{\alpha}\sigma_z; \langle \alpha+1 \rangle_x, (\alpha \ \alpha+1)_y, (\alpha \ \alpha+1)_z).$$

If the pipe into which we wish to insert a vertex has zero length, such a map may insert a vertex coincident to an existing one. This poses no problem in the discriminant, but would result in a knot mapping to a singular curve. For example, if $v_i = (v_i^x, v_i^y, v_i^z)$, and $v_{i+1} = (v_i^x, v_i^y, v_{i+1}^z)$, inserting a vertex in either of \mathbf{x}_i or \mathbf{y}_i results in $\iota_n^{good}(v)_i = \iota_n^{PL}(v)_{i+1} = v_i$, so $\iota_n^{good}(v) \left(\frac{3i+1}{n} \right) = \iota_n^{good}(v) \left(\frac{3i+4}{n} \right)$, an intersection of distant pipes.

We resolve this issue by borrowing length from the two surrounding pipes, at least one of which is guaranteed to have non-zero length if the curve is non-singular. In some cases, this requires changing the coordinates of the two existing neighboring vertices in a manner which does not change the knot type of the image, as in Figure 5. To ensure that we don't change the knot type, we limit our deformation of the knot in either borrowing direction to half the distance to the closest pipe, which must run perpendicular to the plane in which the two vertices occur.

Notice that this issue only arises if two specific consecutive vertices in the curve lie in the same coordinate plane. These are precisely the curves produced by points lying in the closure of codimension 1 cells named $e(\sigma_x, \sigma_y, \sigma_z; (\alpha \ \alpha+1)_{e_{[n]_3}})$. Call any such cell α -planar. All cells which are neither good nor α -planar, those for which $(\alpha \ \alpha+1)$ appears in $\sigma_{[n]_3}$ but which are not in the closure of an α -planar cell will be called *interpolating*.

We make the following sequence of definitions for $e_{[n]_3} = x$. Similar definitions can be made for y and z .

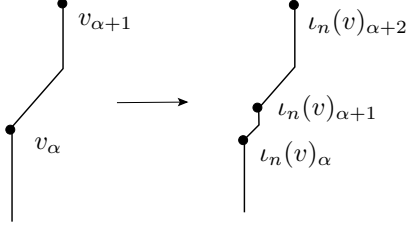
Definition 3.4. Let $\alpha(n)$ and α be as in Definition 3.2 and $v \in e \in \text{CELL}_{\bullet}(P_n)$ with e an α -planar cell

Define $\iota_n^P(v)$ by

$$(\iota_n^P(v))_i = \begin{cases} v_i & i \leq \alpha - 1 \\ (v_{\alpha}^x, v_{\alpha}^y, \frac{1}{2}(v_{\alpha}^z + v_{\sigma_z(\sigma_z^{-1}(\alpha) + s(\mathbf{z}_{\alpha-1}))}^z)) & i = \alpha \\ (v_{\alpha}^x, \frac{1}{2}(v_{\alpha}^y + v_{\sigma_y(\sigma_y^{-1}(\alpha) + s(\mathbf{y}_{\alpha}))}^y), v_{\alpha}^z) & i = \alpha + 1 \\ v_{i-1} & i \geq \alpha + 2. \end{cases}$$

ι_n^P is a cellular map from α -planar cells to the barycentric subdivision of the codomain.

Lemma 3.5. Let $e \in \text{CELL}_{\bullet}(P_n)$ be an α -planar cell. Then the image of e under the induced chain map $(\iota_n^P)_{\#}$ is

FIGURE 5. $\iota_n^P(v)$

$$(\iota_n^P)_\#(e(\sigma_x, \sigma_y, \sigma_x; (\alpha \ \alpha+1)_x)) = e(j_{\alpha, \alpha+1} \sigma_x, j_\alpha \sigma_y, j_\alpha \sigma_z; (\alpha \ \alpha+1)_x \langle \alpha+1 \rangle_x, \langle \alpha+1 \rangle_y, \langle \alpha+1 \rangle_z).$$

It now remains to continuously extend the maps ι_n^{good} and ι_n^P across the interpolating cells. When within such a cell, rather than just inserting a vertex we will also slightly perturb the vertices using the borrowing construction from Definition 3.4. See Figure 6 for an example of how the map functions on a point which requires such an interpolation.

Definition 3.6. Let $\alpha(n)$ and α be as in Definition 3.2 and $v \in e \in \text{CELL}_\bullet(P_n)$ with e an interpolating cell.

We define the interpolating parameter $p(v)$ to be the ratio of the distance between v_α^x and $v_{\alpha+1}^x$ to the maximal distance between them within the cell if we fix the other vertices.

$$p(v) = \frac{\|\mathbf{x}_\alpha\|}{|v_{\sigma_x(\sigma_x^{-1}(\alpha)-s(\mathbf{x}_\alpha))}^x - v_{\sigma_x(\sigma_x^{-1}(\alpha+1)+s(\mathbf{x}_\alpha))}^x|}$$

Define $\iota_n^I(v)$ by

$$(\iota_n^I(v))_i = \begin{cases} v_i & i \leq \alpha - 1 \\ (v_\alpha^x, v_\alpha^y, v_\alpha^z - \frac{p(v)}{2}(v_\alpha^z - v_{\sigma_z(\sigma_z^{-1}(\alpha)+s(\mathbf{z}_{\alpha-1}))}^z)) & i = \alpha \\ (v_\alpha^x, v_\alpha^y - \frac{p(v)}{2}(v_\alpha^y - v_{\sigma_y(\sigma_y^{-1}(\alpha)+s(\mathbf{y}_\alpha))}^y), v_\alpha^z) & i = \alpha + 1 \\ v_{i-1} & i \geq \alpha + 2. \end{cases}$$

Now, we define ι_n as the union of these three maps. For $m > n$, write $\iota_{n,m} = \iota_{m-1} \circ \iota_{m-2} \circ \dots \circ \iota_n$ and $\iota_{n,n}$ the identity.

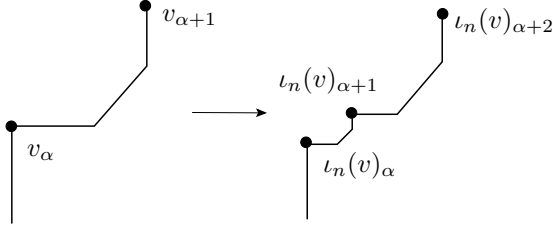
Only ι_n^I fails to be cellular in any sense, though the image of an interpolating cell is contained in a cell we can name.

Lemma 3.7. *Let $\alpha = \alpha(n) + 1$ and e an interpolating cell. The image of e under ι_n^I satisfies*

$$\iota_n^I(e(\sigma_x, \sigma_y, \sigma_x)) \subseteq e(j_{\alpha, \alpha+1} \sigma_x, j_\alpha \sigma_y, j_\alpha \sigma_z; \langle \alpha + 1 \rangle_x).$$

Now, as we have been careful in our definitions, the following lemma is immediate.

Lemma 3.8. $\iota_n : K_n \hookrightarrow K_{n+1}$ and $\iota_n : S_n \hookrightarrow S_{n+1}$.

FIGURE 6. $\iota_n^I(v)$

That is, the $\{K_n\}$ form a directed system under the ι_n . Let $\iota_{n,\infty} : K_n \rightarrow \varinjlim K_n$ be the induced map. Similarly for S_n .

Definition 3.9. Let $v \in K_n$ and $w \in K_m$. We say ϕ_v and ϕ_w are *isotopic* if there is a path $\bar{\Phi}_{v,w} : \mathbb{I} \rightarrow \varinjlim K_n$ with $\bar{\Phi}(0) = \iota_{n,\infty}(v)$ and $\bar{\Phi}(1) = \iota_{m,\infty}(w)$.

It follows from Lemma 3.8 that if ϕ_v and $\phi_w \in K_n$ are geometrically isotopic, so are $\phi_{\iota_n(v)}$ and $\phi_{\iota_n(w)}$.

We wish to compare these new spaces K_n to more familiar spaces of (long) knots. We will use PL maps of n segments whose segments are each parameterized by intervals of fixed length $\frac{3}{n}$, so the i th segment has domain $[\frac{3i}{n}, \frac{3(i+1)}{n}]$. Given a point $v \in (\text{Int } \mathbb{I}^3)^{n-1}$, a *PL map* of “ n segments” is a map $\psi_v : \mathbb{R} \rightarrow \mathbb{R}^3$ with support on $[0, 3]$, built in a manner similar to that for a plumbers’ curve.

Definition 3.10. Let $v \in (\text{Int } \mathbb{I}^3)^{n-1}$, and for $i \in \{0, \dots, n-1\}$ construct linear maps between consecutive v_i as follows.

$$\ell_i(t) : \left[\frac{3i}{n}, \frac{3(i+1)}{n} \right] \rightarrow \mathbb{R}^3 = (3i+1-nt)v_i + (nt-3i)v_{i+1}$$

Each such map is a *segment*, and as with pipes we will sometimes fail to distinguish between the map and its image. Let $\psi_v : [0, 3] \rightarrow \mathbb{R}^3$ be the union of the ℓ_i , so for t in the domain of ℓ_i , $\psi_v(t) = \ell_i(t)$. Such a map is a *PL map with n segments*.

Definition 3.11. Let $v \in (\text{Int } \mathbb{I}^3)^{n-1}$ and ψ_v a PL map with n segments. ψ_v is *non-singular* if $\psi_v(s) = \psi_v(t)$ only if $s = t$. A non-singular PL map with n segments is a *PL knot with n segments*. Denote space of all such maps by L_n .

The maps which make L_n into a directed system are constructed in a manner similar to the maps between the P_n , but are much more straightforward, defined simply to be “inserting a vertex in the middle of the $\alpha(n)$ th move”. This requires a reparameterization of the map in order to make it a valid element of L_{n+1} , which we produce by reconstructing the knot from the new list of vertices.

Definition 3.12. Let $\alpha(n), \alpha$ be defined as before. For $v \in (\text{Int } \mathbb{I}^3)^{n-1}$, define

$$(I_n(v))_i = \begin{cases} v_i & i < \alpha \\ \frac{1}{2}(v_{i-1} + v_i) & i = \alpha \\ v_{i-1} & i > \alpha. \end{cases}$$

It is apparent that I_n is injective for all n . For $m > n$, write $I_{n,m} = I_{m-1} \circ I_{m-2} \circ \dots \circ I_n$, $I_{n,n}$ is the identity. The spaces $\{L_n\}$ form a directed system under I_n , so let $\iota_{n,\infty} : L_n \rightarrow \varinjlim L_n$ be the induced map.

Geometric isotopy and isotopy of PL knots are defined in precisely the same manner as for plumbers' knots.

Let \mathcal{K} be the space of C^1 long knots in \mathbb{R}^3 . With the construction we have exhibited, it is known that $\pi_0(\varinjlim L_n) \cong \pi_0(\mathcal{K})$. We wish to establish that $\pi_0(\varinjlim K_n) \cong \pi_0(\varinjlim L_n)$ in order to use the space of plumbers' knots as a model for studying isotopy classes of knots in \mathcal{K} . Our method for proving this fact, stated in Theorem 3.17, is standard but technically difficult: we produce maps from each directed system to the other which are, up to isotopy, inverses in the limit.

To simplify the proof of this theorem, we will want to be able to say that a map from one space of knots to another “respects the isotopy type” of a knot. To make this rigorous, we approximate both PL and plumbers' knots with C^1 knots and compare these approximations, thus allowing us to compare C^1 -isotopy classes across knot spaces. It is known that we can approximate a PL knot $\psi_w \in L_n$ to arbitrary precision with a C^1 knot $\psi_{\tilde{w}}$ via a careful choice of corner smoothing, so it remains to do the same with plumbers' knots. This approximation will not be canonical, but it is well defined on components of the space.

We proceed by producing an appropriate map $K_n \rightarrow L_{3n}$. We would like to use the naive map that sends a plumbers' knot to the PL knot defined by the same set of vertices. However not all plumbers' knots consist of vertices which produce valid PL knots, as plumbers' knots can have up to two consecutive pipes of zero length. In order to produce continuous maps, we rely on techniques similar to those used to produce maps between the K_n , “buckling” knots which have segments whose length is below a particular threshold.

Definition 3.13. Let $v \in K_n$. Define the *global perturbation distance* $\epsilon(v)$ for the knot ϕ_v to be a small fraction of the minimum of the distances between distant pipes and between pipes which do not intersect the boundary of the unit cube and that boundary. By perturbing the knot no more than this distance, we are sure not to change the isotopy type or make it singular.

Define the *buckling* function for a pipe p in ϕ_v by

$$\beta(p) = \begin{cases} \sqrt{\frac{\epsilon(v)^2 - \|p\|^2}{2}} & \epsilon > \|p\| \\ 0 & \epsilon \leq \|p\|. \end{cases}$$

The buckling function acts as the borrowing function did before, providing an interpolation which allows us to make our function continuous. As the length of a particular pipe shrinks, we deform the the image of the knot in L_{3n} by moving the vertices at its endpoints into the pipes which neighbor it, as in Figure 7.

Produce a map $f_n : K_n \rightarrow L_{3n}$. For each $i \in \{0, \dots, n-1\}$ define

$$\begin{aligned} (f_n(v))_{3i} &= (v_i^x + s(\mathbf{x}_i)\|\mathbf{x}_i\|\beta(\mathbf{z}_{i-1}), v_i^y, v_i^z - s(\mathbf{z}_{i-1})\|\mathbf{z}_{i-1}\|\beta(\mathbf{x}_i)), \\ (f_n(v))_{3i+1} &= (v_i^x - s(\mathbf{x}_i)\|\mathbf{x}_i\|\beta(\mathbf{y}_i), v_i^y + s(\mathbf{y}_i)\|\mathbf{y}_i\|\beta(\mathbf{x}_i), v_i^z), \\ (f_n(v))_{3i+2} &= (v_i^x, v_i^y - s(\mathbf{y}_i)\|\mathbf{y}_i\|\beta(\mathbf{z}_i), v_i^z + s(\mathbf{z}_i)\|\mathbf{z}_i\|\beta(\mathbf{y}_i)). \end{aligned}$$

Here, for convenience, define $\beta(\mathbf{z}_{-1}) = \|\mathbf{z}_{-1}\| = 0$.

The image of f_n has the property that $|f_n(v)(t) - v(t)| < \epsilon(v)$. We now approximate $\psi_{f_n(v)}$ by a C^1 knot $\widetilde{\psi_{f_n(v)}}$ within $\epsilon(v)$ in order to obtain an approximation of ϕ_v .

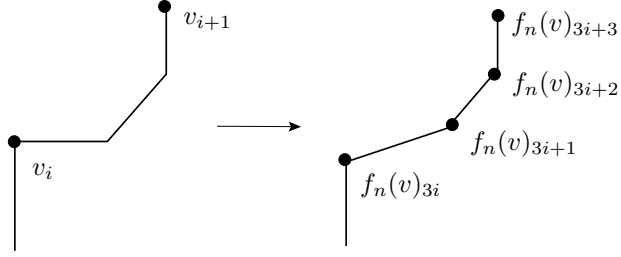


FIGURE 7. Buckling a plumbers' knot to create a PL knot

Definition 3.14. Let $g : K_n \rightarrow L_m$ (respectively $h : L_m \rightarrow K_n$). We say g *respects the knot type of ϕ_v* if $\psi_{\widetilde{f_n(v)}}$ is isotopic to $\psi_{g(v)}$ in \mathcal{K} (respectively $\phi_{\widetilde{f_m(h(v))}}$ is isotopic to $\phi_{\bar{v}}$). If g respects the knot type of all ϕ_v , we say g *respects knot types*.

We will make use of the maps f_n in our proof of Theorem 3.17. The inverse maps are defined as follows:

Definition 3.15. Let $w \in L_n$. Define $A_n : L_n \rightarrow K_n$ to be the map which takes the PL knot ψ_w to the plumbers' knot ϕ_w . In general, A_n does not preserve knot types or even non-singularity. However, in order to ensure that A_n respects knot type it is sufficient to force the lengths of segments in ψ_w to be sufficiently small.

Define the *maximal segment length function* δ for $w \in L_n$ by

$$\begin{aligned} m_1 &= \min\{d(\ell_i, \ell_j) \mid |i - j| > 1\} \\ m_2 &= \min\{d(w_i, \partial(\mathbb{I}^3)) \mid i \in \{1, \dots, n-1\}\} \\ \delta(w) &= \frac{1}{10} \min(m_1, m_2). \end{aligned}$$

Let $N(w)$ be the minimum number so that $\psi_{I_{n,N(w)}(w)}$ is a PL knot with the property that no segment has length greater than $\delta(w)$.

Lemma 3.16. $A_{N(w)} \circ I_{n,N(w)}$ respects the knot type of ψ_w .

Theorem 3.17. The induced map $f_* : \pi_0(\varinjlim K_n) \rightarrow \pi_0(\varinjlim L_n)$ is an isomorphism of sets.

Proof. Let $\bar{w} \in \varinjlim L_n$ and k an integer and $w \in L_k$ so that $I_{k,\infty}(w) = \bar{w}$. We require that in following family of diagrams indexed by \bar{w} , the images of ψ_w under both paths are geometrically isotopic.

$$\begin{array}{ccccc} & & I_{k,3N(w)} & & \\ & \nearrow & & \searrow & \\ L_k & \xrightarrow{I_{k,N(w)}} & L_{N(w)} & & L_{3N(w)} \\ & \searrow & \downarrow A_{N(w)} & \nearrow f_{N(w)} & \\ & & K_{N(w)} & & \end{array}$$

However, as A_n , f_n and I_n respect the knot type of ψ_w , there is a geometric isotopy between the images. Since the ι_n are injective, this says that for $\bar{w} \in \varinjlim L_n$ there exists $\bar{v} \in \varinjlim K_n$ which maps to the isotopy class of $\psi_{\bar{w}}$ under f_* .

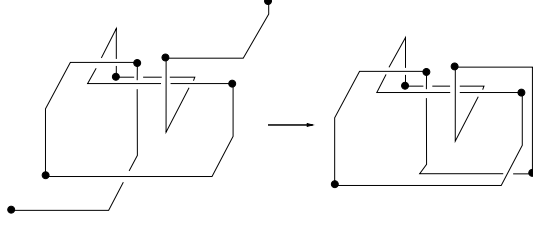


FIGURE 8. Closing a plumbers' knot to obtain a lattice knot.

Now, let $\psi_{\bar{w}}$ and $\psi_{\bar{w}'}$ be isotopic elements of $\varinjlim L_n$. We can lift an isotopy between them to a geometric isotopy at some finite stage, $\Psi_{w,w'} : \mathbb{I} \rightarrow L_n$. Let $N = \max\{N(\Psi(t)) \mid t \in \mathbb{I}\}$, where $N(w)$ is as in Definition 3.15. Precompose $\Psi_{w,w'}$ by $I_{n,N}$ to produce a geometric isotopy $\hat{\Psi}$ between $\psi_{I_N(w)}$ and $\psi_{I_N(w')}$. Now we can apply A_N to get a geometric isotopy between $\phi_{(A_N \circ I_N)(w)}$ and $\phi_{(A_N \circ I_N)(w')}$. Per the proof of surjectivity, under f_N these map to elements geometrically isotopic to $\psi_{I_{3N}(w)}$ and $\psi_{I_{3N}(w')}$ respectively. That is, if $\psi_{\bar{w}}, \psi_{\bar{w}'} \in \varinjlim L_n$ are isotopic, we can construct an isotopy between elements of $\varinjlim K_n$ which map to knots isotopic to $\psi_{\bar{w}}$ and $\psi_{\bar{w}'}$, so f_* is injective. \square

The homotopy types of the components of $\varinjlim K_n$ almost certainly differ from those of $\varinjlim L_n$. It seems possible that, a model similar to this one can be constructed which has the homotopy type of the space of C^1 long knots. As the details are technically complicated and of limited interest to our intended application, no attempt has been made to resolve the question.

4. RELATIONSHIPS WITH LATTICE KNOTS AND CUBICAL DIAGRAMS

We observe that plumbers' knots bear strong resemblance to a number of other knot theories. Two of particular interest are lattice knots and cubical diagrams. Lattice knots are studied because they can be used to model physical data like length and thickness of the material from which a knot is constructed. Cubical diagrams are used in [1] to construct chain complexes of knots with which one can study knot Floer homology.

4.1. Lattice knots. A lattice knot is a PL knot whose segments lie parallel to the coordinate axes and meet one another on points of the integer lattice $\mathbb{Z}^3 \subseteq \mathbb{R}^3$. Clearly, such knots are very closely related to the representative knots of Definition 2.11. In fact, any representative of a cell of non-singular plumbers' knots can be "closed" to produce a lattice knot, as in Figure 8.

Definition 4.1. Recall that L_m is the space of m -segment piecewise linear knots and suitably modify the definitions given so that maps in L_m have their images in $[0, N]^3$ for some large N . Let $Lat_m \subseteq L_m$ be the subspace of lattice knots.

Let $\phi_v \in P_n$ be a representative knot for the cell $e(\sigma_x, \sigma_y, \sigma_z)$ and define a lattice knot $LK(\phi_v) \in Lat_{3n-1}$ by

$$\begin{aligned}
LK(v)_0 &= (n+1, n \cdot v_{n-1}^y, 0) \\
LK(v)_1 &= (n \cdot v_1^x, n \cdot v_{n-1}^y, 0) \\
LK(v)_2 &= (n \cdot v_1^x, n \cdot v_1^y, 0) \\
\\
LK(v)_{3k} &= (n \cdot v_k^x, n \cdot v_k^y, n \cdot v_k^z) \\
LK(v)_{3k+1} &= (n \cdot v_{k+1}^x, n \cdot v_k^y, n \cdot v_k^z) \\
LK(v)_{3k+2} &= (n \cdot v_{k+1}^x, n \cdot v_{k+1}^y, n \cdot v_k^z) \\
\\
LK(v)_{3n-3} &= (n \cdot v_{n-1}^x, n \cdot v_{n-1}^y, n \cdot v_{n-1}^z) \\
LK(v)_{3n-2} &= (n+1, n \cdot v_{n-1}^y, n \cdot v_{n-1}^z)
\end{aligned}$$

where k ranges from 1 to $n-2$.

Each representative knot for a codimension 0 cell of P_n maps to a lattice knot with $3n-1$ segments. However, these knots tend to use more segments than necessary and there is some interest in discovering the minimal number of segments required to create a lattice knot of a given topological knot type. Recall that, as in Definition 2.11, the idea of a representative knot is extensible to cells of any dimension in $\text{CELL}_\bullet(K_n)$. As some of the plumbers' knots what appear in these cells contain zero-length pipes which must be omitted from their image in Lat_m , we can study them as a means to find lattice knots with fewer segments. A pipe has zero length precisely when the two vertices which define its move are in the same appropriate coordinate plane.

Proposition 4.2. *Let $\rho \in \Sigma_n$ and define $\mu(\rho)$ to be the number of pairs of consecutive integers which appear in the same cycle in ρ . Let $v \in e(\sigma_x, \sigma_y, \sigma_z; \rho_x, \rho_y, \rho_z)$. The number of zero-length pipes in ϕ_v is $\mu(v) = \mu(\rho_x) + \mu(\rho_y) + \mu(\rho_z)$.*

Also, notice that when we close an n -move plumbers' knot for which $v_1^y = v_{n-1}^y$, there is a zero length segment produced in the closure. This occurs when 1 and $n-1$ appear in the same cycle in ρ_y .

Further, since adjacent pipes can move along the same coordinate axis, it is permissible to omit a vertex in the middle of the segment when we construct the lattice knot.

Proposition 4.3. *Let $\rho \in \Sigma_n$ and $\nu(x)$ the number of pairs of consecutive integers which appear in the same cycle in ρ_y and ρ_z . Let $v \in e(\sigma_x, \sigma_y, \sigma_z; \rho_x, \rho_y, \rho_z)$. The number of consecutive moves which travel only along single axes in ϕ_v is $\nu(v) = \nu(x) + \nu(y) + \nu(z)$.*

Notice that if ϕ_v is a plumbers' knot, the same pair of consecutive integers can never occur in all three of ρ_x , ρ_y and ρ_z , as this would produce three consecutive zero-length pipes.

Lemma 4.4. *For $v \in K_n$, $\mu(v) + \nu(v) + \delta_{v_1^y, v_{n-1}^y} \leq 3(n-2) + 1$.*

Definition 4.5. Let $\phi_v \in K_n$ be a representative knot for $e(\sigma_x, \sigma_y, \sigma_z; \rho_x, \rho_y, \rho_z)$ and $\mu(v)$ and $\nu(v)$ as above. Define a lattice knot $LK(v) \in \text{Lat}_{3n-1-\mu(v)-\nu(v)}$ in the same manner as in Definition 4.1, omitting vertices which would coincide or which bound two segments which move along the same coordinate axis.

Using this definition, Lemma 4.4 says that the smallest number of segments that can occur in a lattice knot arising as the closure of a plumbers' knot of n moves

is 4. Clearly, such a lattice knot is an unknot. This bound is achieved by the representative of the cell $e(12 \dots (n-1)_x, 12 \dots (n-1)_y, 12 \dots (n-1)_z; (1 \ 2 \dots (n-1))_y, (1 \ 2 \dots (n-1))_z)$, for example.

The lattice knots which are produced by plumbers' knots are characterized by one or two segments lying in the $z=0$ plane and one in the plane with the highest x coordinate. Every lattice knot can be deformed to such, under the appropriate notion of isotopy. It seems likely, therefore, that plumbers' knots will serve as a bridge to allow translation of tools from classical knot theory to be applied to finite complexity knot theory and vice versa.

4.2. Remarks on cube diagrams. The cube diagrams of Baldridge and Lowrance [1] are essentially lattice knots restricted in a manner which increases their resemblance to plumbers' knots. Similar to our discussion above, these contain information identical to that in a plumbers' knot representative of a cell. We expect that our development of the combinatorics of plumbers' knots will illuminate computations in the cube diagram chain complex for knot Floer homology. Further, as we study plumbers' knots relationship to finite-type invariants in [3], this may provide a method of understanding connections between the two theories.

REFERENCES

1. S. Baldridge and A. Lowrance, *Cube diagrams and a homology theory for knots*, arXiv:0811.0225v1 [math.GT], 2008.
2. Jorge Alberto Calvo, *Geometric knot spaces and polygonal isotopy*, J. Knot Theory Ramifications **10** (2001), no. 2, 245–267, Knots in Hellas '98, Vol. 2 (Delphi). MR MR1822491 (2002b:57002)
3. C. Giusti, *Unstable Vassiliev theory*, In preparation, 2008.
4. E. J. Janse van Rensburg and S. D. Promislow, *The curvature of lattice knots*, J. Knot Theory Ramifications **8** (1999), no. 4, 463–490. MR MR1697384 (2000i:57009)